TECHNICAL PAPER

On the static analysis of laminated composite frames having variable cross section

Hasibullah Rasooli[1] [iD] · **Ahmad Reshad Noori[2]** · **Beytullah Temel[1]**

Abstract

The complementary functions method (CFM) is used to investigate the static behavior of laminated composite frames consisting of straight and/or curved members of variable cross section. The Timoshenko beam theory (TBT) is used to obtain the set of the governing equations. The fifth-order Runge–Kutta (RK5) algorithm is employed in the solution process of initial value problems via the CFM. A computer program is substantially coded in Fortran on rigidity matrix based on the CFM to acquire the rigidity matrices and load vectors of these structural elements. With the help of the suggested method, the influences of the symmetric layer stacking sequence, the ratio of E_1/E_2, and various boundary conditions on the nodal displacements and element end forces of the considered frames are investigated. Carrying out the static behavior of laminated composite frame systems which contain straight and circular axis elements for the first time by using the CFM is the novelty of this study. Verification and accuracy of the suggested scheme are intently performed through the comparison of the present results with those of the finite element method. The effectiveness of the method and good agreement of the results are observed.

Keywords Laminated composite · Frame structures · Complementary functions method · Two-point boundary value problem · FSDT

1 Introduction

Composite materials are now extensively used in engineering applications due to their transcendent mechanical properties like high mechanical strength, rigidity, corrosion resistance, lightweight, acoustics, fatigue strength, high thermal conductivity, safety, high-temperature resistance and cost-effectiveness. Together with the development of modern engineering and society, complex architectural structures became prevalent. Laminated composite beams are widely

---

✉ Hasibullah Rasooli
  hasibullah.rasooli@gmail.com

  Ahmad Reshad Noori
  arnoori@gelisim.edu.tr

  Beytullah Temel
  btemel@cu.edu.tr

1 Department of Civil Engineering, Çukurova University, Adana, Turkey

2 Department of Civil Engineering, Istanbul Gelisim University, Istanbul, Turkey

used in solving such significant engineering problems and applications; therefore, analysis of laminated composite beams has become a research focus among many engineering disciplines; thus, many papers can be found on its static and dynamic analysis in the literature.

Many solution models and different theories have been developed for the analysis of composite beam structures. Vo and Thai [1] carried out the static analysis of laminated composite beam with various ply lay-ups undergoing uniformly distributed and point loads using a refined shear deformation theory. Ditaranto [2] used a variational method to obtain the differential governing equations and boundary conditions for laminated composite beams with three layers of which the middle layer carries shear forces. Reddy et al. [3] investigated the relationship between deflection, shear forces and bending moments of a third-order shear deformation beam theory and other various beam theories. Karamanlı [4] employed the Timoshenko beam theory and the Ritz method to investigate the bending behavior of composite symmetric and anti-symmetric cross-ply beams under various sets of boundary conditions. Catapano et al. [5] carried out the linear static analysis of simply supported composite cross-ply beams subjected to bending loads considering different

length-to-thickness ratio values and implemented a closed-form Navier-type solution. The results obtained are validated with those of the three-dimensional finite element (FE) models in the ANSYS program. Özütok and Madenci [6] used a higher-order shear deformation beam theory to analyze the static behavior and shear deformation effects in the thickness direction of laminated composite beams with various boundary conditions. Pagani et al. [7] carried out the exact static response of a simply supported cross-ply laminated composite sandwich beam under sinusoidal loading by using a refined beam model based on the Lagrange expansion. Ecsedi and Baksa [8] have developed an analytical model to study the static response of a two-layered composite beam with an interlayer slip in which the loading acts on the symmetry plane of the beam. Euler Bernoulli's theory was supposed to be valid for each layer separately. Aguiar et al. [9] presented several FE models to investigate the static behavior of laminated composite beams of various cross sections. The governing equations were obtained by utilizing the Hellinger–Reissner variation principle. Eisenberger [10] has obtained the exact stiffness coefficients for high-order isotropic beam elements under different in-plane loading and various boundary conditions, and the results were validated with the Timoshenko and Bernoulli–Euler beam theories. Khdeir and Reddy [11] investigated the effects of shear deformation, the number of layers and the E_1/E_2 ratio on the static response of thick and thin cross-ply laminated beams using the first-, second- and third-order beam theories. Yuan and Miller [12] developed a new higher-order FE model to investigate the static response of symmetric and asymmetric laminated composite beams subjected to various boundary conditions. Yu [13] presented a new FE model to analyze the bending response of laminated composite beams and thin plates with different stacking sequences. Vo et al. [14] used a quasi-3D theory in order to investigate the flexural analysis of composite and sandwich beams subjected to various boundary conditions and considering the effects of fiber angle, layer stacking sequences and span to height ratio on the displacements and stresses. Cunedioğlu [15] used the FE method based on Euler–Bernoulli beam theory to study the static and buckling behaviors of a fiber-reinforced composite beam considering various parameters and proved that these parameters significantly influence the displacement and buckling loads of the beam. Masjedi and Weaver [16] presented an analytical solution for the 3D static response of non-uniform composite beams of variable stiffness. The proposed solution is derived by direct integration and series expansion methods. A slender beam with rectangular cross section subjected to tip and uniformly distributed loads, was examined. Daví et al. [17] developed a new theory for multilayered beams under axial, shear and bending loads acting on the ends of the beam. Their suggested model was applied on a single-layer beam to compare the accuracy of the

results; thereafter, closed-form solutions were given for beams subjected to various supports and loading conditions. Vukasovic et al. [18] modified classical Timoshenko beam theory to investigate the influence of shear on thin-walled laminated composite beams of symmetrically open cross sections subjected to uniformly distributed loads and various boundary conditions. Saraçoğlu et al. [19] studied the deflection response of fiber-reinforced orthotropic beams according to the Bernoulli–Euler and Timoshenko beam theories. The influence of the length to depth ratio, material properties and fiber orientation angle on deflection was also examined in detail. An FE model based on the first-order shear deformation and Timoshenko beam theories was developed by Elshafei [20] to analyze the behaviors of isotropic and orthotropic beams. Besides, the effect of thickness to length ratio, material properties, boundary conditions and the number of layers on the natural frequency and the static deflections of the beam were investigated. Zghal et al. [21] investigated the effects of porosity, boundary conditions, porosity coefficient and porosity distribution types on bending response of functionally graded (FG) beams using a refined mixed FE beam model. Doeva et al. [22] introduced an exact analytical solution for static deformation analysis of composite beams subjected to non-uniformly distributed loads and various boundary conditions. Noori et al. [23] used the CFM to study the static bending of FG straight beams of variable mechanical and material properties through the thickness, subjected to different boundary conditions and various in-plane loads. Mathiyazhagan and Vasiraja [24] used an FE formulation to study the influence of loading type and direction on the static deflection of a cantilever curved beam of various cross sections. Barhate and Waghe [25] developed various theories to study the static analysis of simply supported and laminated composite beams loaded transversely. Alaimo et al. [26] introduced an analytical theory to analyze the axial and transverse displacements of multilayered composite beams under uniformly distributed loads acting transversely. Sayyad et al. [27] investigated the effects of shear transverse deformation on the bending response of laminated composite and sandwich beams using a trigonometric beam theory, which does not require a shear correction factor. Pandey and Gadade [28] statically analyzed laminated composite beams undergoing transverse loads considering aspect ratios, ply lay-up and boundary conditions through a well-established higher-order shear deformation theory (HSDT). Sayyad and Ghugal [29] proposed a trigonometric beam theory (TBT) to investigate the effects of transverse shear deformation and normal strains on the flexure response of symmetric and anti-symmetric laminated composite beams. Rasooli and Temel [30] carried out the static response of laminated composite beams subjected to the various point and uniformly distributed loads under different boundary conditions. Ghugal and Shinde [31] used a layerwise shear deformation

theory to study the flexural behavior of composite cross-ply laminated beams of fixed and simply supported boundary conditions under sinusoidal loads. Aslan et al. [32] used the CFM to investigate the static analysis of circular axis elements subjected to static transverse concentrated and uniformly distributed loads with various boundary conditions. Karacam and Tımarcı [33] used third-order shear deformation beam theory to study the bending response of composite cross-ply laminated beams under uniformly distributed loads and various boundaries considering the effects of orthotropicity ratios and L/h ratios. Madenci et al. [34] developed a theoretical procedure to study the bending response of the P-GFRP composite beams. They applied a three-point bending experiment in their work. Madenci and Özütük [35, 36] examined the bending behavior of laminated composite plates with the aid of the mixed finite element method.

There have been plenty of research works found on the analysis of composite beams under various loading types and boundary conditions. Simultaneously, the effects of several parameters on the analysis of beam elements are investigated extensively. Even though the frame systems consisting of straight and curved axis beams are vastly used in various real-life engineering applications still, there is not enough research on the analysis of these structural elements. A first-time attempt on the static analysis of the composite laminated frame systems containing straight and curved axis elements with variable cross sections through an efficient and easy applicable numerical approach expresses the novelty of this paper. The CFM was applied successfully in structural mechanics [37–44]. Using the CFM based on the rigidity matrix is also a novelty of this paper.

The main objective of this paper is to improve the CFM for the static analysis of laminated composite frame systems that comprise straight and curved beam elements with variable cross sections along the axial direction. The influences of boundary conditions, layer stacking angle and the E_1/E_2 ratio on the bending deflection and rotation of the system are investigated extensively. The differential equations that govern the static response of these structures are obtained with the help of Timoshenko's beam theory. The RK5 algorithm is applied in numerical calculations. For this purpose, a computer program is coded in Fortran. For validation, accuracy and applicability of the present method, a frame system consists of composite laminated beam elements with a uniform cross section and various static loading is analyzed numerically and the results obtained are compared with those of the FEM-based results obtained from ANSYS [45].

A brief outline for a better presentation of the paper is in the following order: Sect. 2 prescribes the mathematical formulation, derivation of the canonic differential equations and theory of the proposed approach. Section 3 presents the effects of fiber angle, orthotropicity ratio, boundary conditions and material properties on the static analysis of variable cross-sectional frame systems with the help of the proposed method. Section 4 of the paper is devoted to the discussion of the overall investigation of this research.

2 Theory and formulations

2.1 Governing equations

Choosing the $\vec{t}, \vec{n}, \vec{b}$ moving coordinate system provides big ease during formulations within the scope of this framework. Here $\vec{t}$ is tangent unit vector and $\vec{n}, \vec{b}$ are normal and binormal unit vectors [46].

$$\vec{r} = \vec{r}(s); \vec{t} = \frac{d\vec{r}}{ds}; \vec{b} = \vec{t} \times \vec{n} \tag{1}$$

The above relations can be written according to Fig. 1.

The relationship between these $\vec{t}, \vec{n}, \vec{b}$ unit vectors is obtained by using the Frenet formulas in the following form.

$$
\begin{aligned}
\frac{d\vec{t}}{ds} &= \chi \cdot \vec{n} \\
\frac{d\vec{n}}{ds} &= \tau \cdot \vec{b} - \chi \cdot \vec{t} \\
\frac{d\vec{b}}{ds} &= -\tau \cdot \vec{n}
\end{aligned}
\tag{2}
$$

In the given equations χ and τ denote the curvature and twisting of the curved element of which relation can be written as $= \frac{1}{R(\phi)}$ and $\tau = 0$ for planar curved axis beam element. The following equations can be written due to simplifying the equilibrium conditions, compliance equations and the constitutive law in the vector form.

$$\frac{d\vec{T}}{ds} + \vec{p} = 0 \tag{3}$$

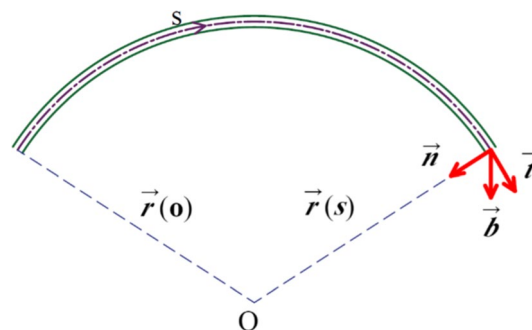$$\frac{d\vec{M}}{ds} + \vec{t} \times \vec{T} + \vec{m} = 0 \tag{4}$$

Fig. 1 Geometry of the element

$$\frac{d\vec{\Omega}}{ds} - [D]^{-1}\vec{M} = 0 \tag{5}$$

$$\frac{d\vec{U}}{ds} + \vec{t} \times \vec{\Omega} - [C]^{-1}\vec{T} = 0 \tag{6}$$

In the above equations, four vector quantities $\vec{T}$ and $\vec{M}$ the internal forces, $\vec{U}$ and $\vec{\Omega}$ the displacement and rotations should be calculated, in order to perform these calculations in an easy way the aforementioned vector equations should be transformed to the scalar form (see [43] for the transformation processes). The $ds = Rd\phi$ relation is accepted for curved elements. After all these transformation procedures are done, the canonical equations for the straight and circular axis beam element can be obtained in the scalar form as follows.

$$\frac{dU_t}{d\phi} = U_n + RA'_{11}T_t \tag{7}$$

$$\frac{dU_n}{d\phi} = -U_t + R\Omega_b + RA'_{22}T_n \tag{8}$$

$$\frac{d\Omega_b}{d\phi} = RD'_{33}M_b \tag{9}$$

$$\frac{dT_t}{d\phi} = T_n - Rp_t \tag{10}$$

$$\frac{dT_n}{d\phi} = -T_t - Rp_n \tag{11}$$

$$\frac{dM_b}{d\phi} = -RT_n - Rm_b \tag{12}$$

The governing equations for straight axis laminated composite beam elements.

$$\frac{dU_t}{dx} = A'_{11}T_t \tag{13}$$

$$\frac{dU_n}{dx} = \Omega_b + \alpha_n A'_{22}T_n \tag{14}$$

$$\frac{d\Omega_b}{dx} = D'_{33}M_b \tag{15}$$

$$\frac{dT_t}{dx} = -p_t \tag{16}$$

$$\frac{dT_n}{dx} = -p_n \tag{17}$$

$$\frac{dM_b}{dx} = -T_n \tag{18}$$

The above ordinary differential equations handle the static behavior of the frames consisting of straight and curved axis laminated composite beam elements subjected to in-plane uniformly distributed and concentrated loads. In the above equations, U_t, U_n, Ω_b express tangent/normal deflections and rotation; T_t/T_n and M_b show the axial/shear forces and bending moments at the desired node of the element. A curved element with a constant radius is accepted as a circle; in the above equations, R demonstrates the radius of the circular element, p_t and p_n point to the external loads acting on the element, α_n describes the shear correction factor, and 1.1875 value is used as α_n within this framework. The extensional and bending stiffness matrices are denoted by A'_{11}, A'_{22} and D'_{33}, respectively. These matrices are (3×3) in dimensions and can be obtained from the inverse of the material matrices, which includes the constitutive equations and total rigidity terms [43]. Details of the total compliance matrices A' and D' of composite frames are given in Appendix A.

2.2 Solution procedures of the rigidity matrix based on the CFM

Consider a differential equation as (see [46]).

$$\frac{d\{Y(\phi)\}}{d\phi} = [A(\phi)]_{n \times n}\{Y(\phi)\}_{n \times 1} + \{F(\phi)\}_{n \times 1} \tag{19}$$

where ϕ is the independent variable, $\{Y\}$ is the column matrix of unknown dependent variables, $[A]$ is differential transformation matrix, and $\{F\}$ matrix is populated with loading properties.

Based on the principle that the homogeneous and particular solution of the equation given in (19) is found with the boundary conditions determined at the beginning of the solution interval, independent of the boundary conditions of the problem (see [46]).

$$\{Y(\phi)\} = \sum_{m=1}^{n} C_m\left[U^{(m)}(\phi)\right] + \{V(\phi)\} \tag{20}$$

In the above equation, C_m is the integration constants that can be calculated from the boundary conditions determined at the beginning and end of the problem. $\left[U^{(m)}(\phi)\right]$ and $\{V(\phi)\}$ are the homogeneous and particular solutions, respectively.

$$\frac{\mathrm{d}\{U^{(m)}\}}{\mathrm{d}\phi} = [A]\{U^{(m)}\} \quad (m = 1 \dots n) \tag{21}$$

The above equation should be solved n time for n number initial conditions.

$$\begin{array}{lll}
m = 1 & m = 2 & m = 3 \\
U_1(a) = 1 & U_2(a) = 0 & U_n(a) = 0 \\
U_1(a) = 0 & U_2(a) = 1 & U_n(a) = 0 \\
\dots & \dots & \dots \\
U_1(a) = 0 & U_2(a) = 0 & U_n(a) = 1
\end{array} \tag{22}$$

$\{U^{(m)}\}$ is the solution obtained in the solution region by giving 1 to the mth element and 0 to the others in the unknown $\{U\}$ column matrix.

$$[U(a)] = [I] \tag{23}$$

where $[I]$ is the identity matrix. Equation (24) is the particular solution for the statement given in (19).

$$\frac{\mathrm{d}\{V\}}{\mathrm{d}\phi} = [A]\{V\} + \{F\} \tag{24}$$

$$\begin{array}{l}
m = n \\
V_1(a) = 0 \\
V_2(a) = 0 \\
\dots \\
V_n(a) = 0
\end{array} \tag{25}$$

It is enough to be solved once for the boundary conditions

$$\{V(a)\} = \{0\} \tag{26}$$

Element equation is given as

$$\{p\} = [k]\{d\} + \{f\} \tag{27}$$

where $\{p\}$ is the end forces matrix, $[k]$ is the rigidity matrix $\{d\}$ is the node displacement matrix, and $\{f\}$ is the encastered end forces matrix.

$$\{d\} = \left\{ U_t(\phi_i), U_n(\phi_i), \Omega_b(\phi_i), U_t(\phi_j), U_n(\phi_j), \Omega_b(\phi_j) \right\}^{\mathrm{T}} \tag{28}$$

$$\{p\} = \left\{ T_t(\phi_i), T_n(\phi_i), M_b(\phi_i), T_t(\phi_j), T_n(\phi_j), M_b(\phi_j) \right\}^{\mathrm{T}} \tag{29}$$

$$\{f\} = \left\{ -T_t(\phi_i), -T_n(\phi_i), -M_b(\phi_i), T_t(\phi_j), T_n(\phi_j), M_b(\phi_j) \right\}^{\mathrm{T}} \tag{30}$$

In order to transfer these equations obtained in element coordinate to the system coordinates, the following transformation process needs to be applied.

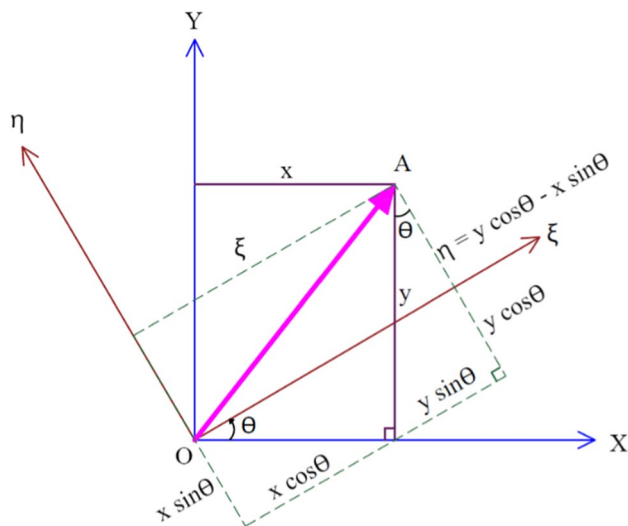$$[k'] = [T]^{\mathrm{T}}[k][T]; \quad [f'] = [T]^{\mathrm{T}}[f] \tag{31}$$

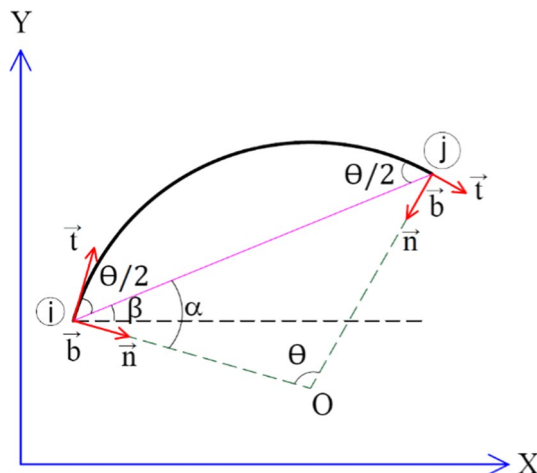**Fig. 2** Coordinate transformation of straight axis element

Fig. 3 Coordinate transformation of curved axis element

The transformation matrix for planar elements is obtained as follows (Figs. 2 and 3) (see [46]):

$$\begin{Bmatrix} \xi \\ \eta \\ z \end{Bmatrix} = \begin{bmatrix} \cos\theta & \sin\theta & 0 \\ -\sin\theta & \cos\theta & 0 \\ 0 & 0 & 1 \end{bmatrix} \begin{Bmatrix} x \\ y \\ z \end{Bmatrix} \tag{32}$$

The transformation relation for i node in $\vec{t}, \vec{n}, \vec{b}$ coordinate system is as

$$t = y\cos(-\alpha) - x\sin(-\alpha), \quad n = x\cos(-\alpha) + y\sin(-\alpha) \tag{33}$$

where

$$\alpha = \frac{\pi}{2} - \frac{\theta}{2} \tag{34}$$

Then in matrix form the statement becomes

$$\begin{Bmatrix} t \\ n \\ b \end{Bmatrix} = \begin{bmatrix} \cos\frac{\theta}{2} & \sin\frac{\theta}{2} & 0 \\ \sin\frac{\theta}{2} & -\cos\frac{\theta}{2} & 0 \\ 0 & 0 & -1 \end{bmatrix} \begin{Bmatrix} x \\ y \\ z \end{Bmatrix} \tag{35}$$

While transferring to system coordinates the equations become as

$$x = X\cos(\beta) + Y\sin(\beta) \tag{36}$$

$$y = Y\cos(\beta) - X\sin(\beta) \tag{37}$$

and in matrix form

$$\begin{Bmatrix} x \\ y \\ z \end{Bmatrix} = \begin{bmatrix} \cos\beta & \sin\beta & 0 \\ -\sin\beta & \cos\beta & 0 \\ 0 & 0 & 1 \end{bmatrix} \begin{Bmatrix} X \\ Y \\ Z \end{Bmatrix} \tag{38}$$

By replacing the above equation in (35) it becomes as

$$\begin{Bmatrix} t \\ n \\ b \end{Bmatrix} = [T]_i \begin{Bmatrix} X \\ Y \\ Z \end{Bmatrix} \tag{39}$$

And for explicit expression of the transformation matrix the following assumption is considered.

$$my = \cos\beta \tag{40}$$

$$ny = \sin\beta \tag{41}$$

and the matrix gets the following form

$$[T]_i = \begin{bmatrix} my\cos\left(\frac{\theta}{2}\right) - ny\sin\left(\frac{\theta}{2}\right) & ny\cos\left(\frac{\theta}{2}\right) + my\sin\left(\frac{\theta}{2}\right) & 0 \\ my\sin\left(\frac{\theta}{2}\right) + ny\cos\left(\frac{\theta}{2}\right) & ny\sin\left(\frac{\theta}{2}\right) - my\cos\left(\frac{\theta}{2}\right) & 0 \\ 0 & 0 & -1 \end{bmatrix} \tag{42}$$

The above matrix is used to provide transformation between element coordinates and system coordinates for i node of the element. The same way by replacing $\left(\frac{\theta}{2}\right)$ with $\left(-\frac{\theta}{2}\right)$ the transformation matrix can be obtained for j node of the element.

$$[T] = \begin{bmatrix} [T]_i & 0 \\ 0 & [T]_j \end{bmatrix}_{6\times6} \tag{43}$$

Boundary conditions considered for each example of this study are given in Table 1.

3 Numerical applications and results discussion

The suggested efficient numerical approach is coded in Fortran to investigate the static analysis of frames with straight and circular axis beam elements. This numerical scheme transforms the two-point boundary value problems into a set of initial value problems. The RK5 algorithm has been applied in the solution of the system of initial value problems. The material properties of both straight and circular axis beam elements are supposed to be varying according to the layer properties in the thickness direction. The proposed procedure is employed to investigate the effects of stacking sequence and orthotropicity ratio on the static behavior of frames systems.

To validate the accuracy of the presented approach, the frame system given in Fig. 5 assumed as uniform cross section and first it is solved with the help of the CFM; subsequently, it is solved by utilizing ANSYS [45].

The material properties taken into account in this study are presented in Table 2. The geometrical model considered

Table 1 Boundary conditions of the problems

Numerical applications	Boundary conditions	At $x=0$	At $x=L$
1. Example	Pinned-clamped (P–C)	$U_t = U_n = M_b = 0$	$U_t = U_n = \Omega_b = 0$
2. Example	Clamped–clamped (C–C)	$U_t = U_n = \Omega_b = 0$	$U_t = U_n = \Omega_b = 0$
3. Example	Roller-clamped (R–C)	$U_n = T_t = M_b = 0$	$U_t = U_n = \Omega_b = 0$

Table 2 Material properties of the structure

Material identity	E_1 (GPa)	$E_2=E_3$ (GPa)	$G_{12}=G_{13}$ (GPa)	G_{23} (GPa)	$v_{12}=v_{13}$	v_{23}	ρ (kg/m³)
Kevlar 49 epoxy	76	5.56	2.3	1.618	0.34	0.718	1460.00
Carbon epoxy	144.8	9.54	4.14	3.45	0.30	0.399	1389.23

for analysis is made of several straight and curved axis laminated composite beam elements with a three-layered rectangular cross section. The cross section of each element is presumed to be variable along the axial direction.

Two-layer layout modules have been considered for the rectangular cross section, the first laminated module (KI) is made of one type of material with three layers, and the second module (KII) is made of two types of material properties with three layers (Fig. 4).

3.1 Example 1

Consider the frame system given in Figs. 5 and 6 with pinned–clamped boundary conditions and subjected to concentrated and uniformly distributed static loads. This probl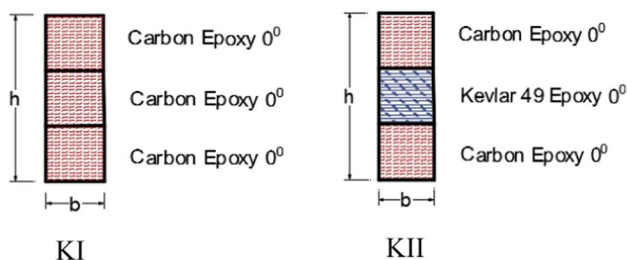em is first analyzed by ANSYS and later by using the suggested scheme for KI material properties (Fig. 4a). The results obtained from both methods are compared as nodal displacements and end forces in Tables 3 and 4, respectively.

Beam 189 element is used while analyzing the problem by ANSYS, and each element of the frame system is divided into 5, 10 and 20 equally parts. This beam element has three nodes with six degrees of freedom (translation in x, y and z directions and rotation about the x-, y- and z-axis) in each node. For more details about the assumptions and restrictions of BEAM189 see Mechanical APDL Element Reference [47] and Mechanical APDL Theory Reference [48]. Separate solutions are carried out for each number of element divisions. Relative error (RE) is calculated by:

$$RE = \left| \frac{ANSYS - peresent\ study}{ANSYS} \right| \tag{44}$$

During the analysis in ANSYS, the KI material properties and 0° of layer angles are used and it is assumed to be constant for each number of element divisions.

The comparison provided in Table 3 reveals that when the mesh quality is increased, the results of the finite element method approach to those of the CFM. This shows the accuracy and efficiency of the suggested method. Also, this method has been applied in the analysis of several structures [37–44] and compared with other available methods like FEM, shooting method.
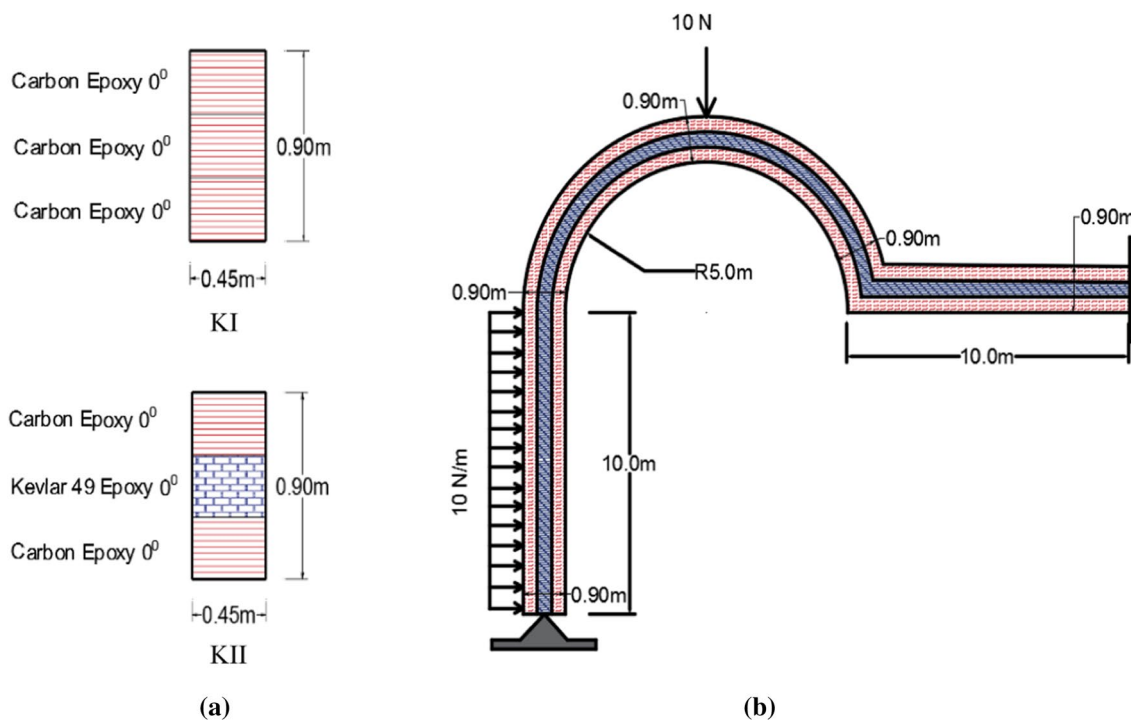

Fig. 4 KI and KII cross-sectional layouts

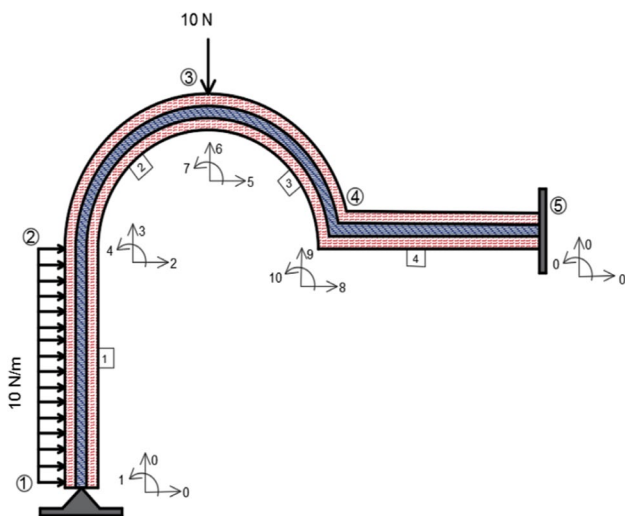**Fig. 5 a** KI and KII cross-sectional layouts and **b** the frame system

Fig. 6 Degrees of freedom of nodes and code numbers

Table 3 Node displacement values for KI group of materials and 0° of fiber angle

Node number	U_t (m)	U_n (m)	Ω_b (Rad.)
1			
ANSYS (5 El.)	0.00000E+00	0.00000E+00	−9.38370E−07
ANSYS (10 El.)	0.00000E+00	0.00000E+00	−9.38720E−07
ANSYS (20 El.)	0.00000E+00	0.00000E+00	−9.38750E−07
Present study	0.00000E+00	0.00000E+00	−9.38618E−07
RE	0.00000E+00	0.00000E+00	1.40632E−04
2			
ANSYS (5 El.)	3.70100E−06	−4.36640E−10	3.64990E−07
ANSYS (10 El.)	3.70420E−06	−4.36350E−10	3.64740E−07
ANSYS (20 El.)	3.70440E−06	−4.36330E−10	3.64720E−07
Present study	3.70257E−06	−4.36357E−10	3.64829E−07
RE	4.94251E−04	6.18759E−05	2.98770E−04
3			
ANSYS (5 El.)	1.53360E−06	1.68460E−06	9.39960E−08
ANSYS (10 El.)	1.53570E−06	1.68250E−06	9.39640E−08
ANSYS (20 El.)	1.53580E−06	1.68250E−06	9.39600E−08
Present study	1.53462E−06	1.68219E−06	9.40191E−08
RE	7.68920E−04	1.84284E−04	6.28596E−04
4			
ANSYS (5 El.)	6.96920E−09	8.21280E−07	−3.00190E−07
ANSYS (10 El.)	6.96880E−09	8.20890E−07	−3.00150E−07
ANSYS (20 El.)	6.96880E−09	8.20870E−07	−3.00140E−07
Present study	6.96890E−09	8.21324E−07	−3.00123E−07
RE	1.43495E−05	5.52766E−04	5.66434E−05

The relative error between the results of the presents approach and those of the ANSYS is calculated in Table 3. The end forces value for each element is given with precision of four digits in Table 4. These results are obtained due

to dividing every single element of the frame system into 20 equal parts and KI material properties with the 0° layer sequences in FEM-based ANSYS program. The values of nodal displacement and element end forces obtained from ANSYS and the present method are seen to be in a good agreement with each other. This verification example demonstrates the accuracy of the suggested numerical method.

3.2 Example 2

Consider a frame system consisting of only straight elements (Figs. 7 and 8) which undergoes the concentrated and uniformly distributed loads subjected to clamped–clamped (C–C) boundary conditions. This frame system is solved by using the present approach considering the effects of layer stacking angles and for both KI and KII material properties. The effects of four different layer stacking angles on the nodal deflection of the given frame system are investigated on both cross section made of KI and KII materials group (Figs. 9 and 10).

Effects of layer stacking angle on the nodal displacements of the frame system (Figs. 7 and 8) are investigated considering KI material properties. The axial and normal displacements and rotations of node 1 and 4 are assumed to be zero due the C–C boundary conditions. Node displacement value for nodes 2 and 3 is calculated considering four different stacking sequences, and the results are obtained with a six-digit precision. After a look on the data in Table 5, it can be seen that the maximum displacement occurred in case III.

The values presented in Table 6 are resulting from solving the frame system (Figs. 7 and 8) for four different cases (Figs. 9 and 10) considering KII material properties. Effects of layer stacking angles on the node displacements and rotation of the system are investigated. When the results are examined, it is understood that the maximum displacement is occurred in case III.

Consider example 2 (Figs. 7 and 8), to investigate the effects of E_1/E_2 ratio on the static behavior of the system, the frame system is solved by the CFM considering KI and KII material properties and four different cross section with various layer stacking angles (Figs. 9 and 10). The system is solved for 1, 10, 15, 20 and 30 ratios of E_1/E_2 with the help of suggested method. This analysis is carried out for both KI and KII material properties by the CFM, respectively. The E_1/E_2 ratios are calculated, by changing the value of E_2 and keeping the value of E_1 as constant. The values of shear modulus are calculated with the help of the following formulations (see Ref. [49, 50]).

$$G_{12} = G_{13} = \frac{E_1}{2\left(\frac{E_1}{E_2} + v_{12}\right)} \tag{45}$$

Table 4 Element end forces obtained for KI materials group and 0° of fiber angle

| Element no	T_{ti}(N)	T_{ni}(N)	M_{bi}(N m)	T_{tj}(N)	T_{nj}(N)	M_{bj}(N m)
1						
Present study	− 59.1316	2.5590	0.0000	− 40.8684	− 2.5590	91.3161
ANSYS	− 59.1320	2.5588	0.0000	− 40.8680	− 2.5588	91.3210
2						
Present study	40.8684	2.5590	− 91.3161	− 40.8684	− 2.5590	− 100.2310
ANSYS	40.8680	2.5588	− 91.3210	− 40.8680	− 2.5588	− 100.2200
3						
Present study	40.8684	− 7.4410	100.2310	− 40.8684	7.4410	66.9058
ANSYS	40.8680	− 7.4412	100.2200	− 40.8680	7.4412	66.9090
4						
Present study	40.8684	− 7.4410	− 66.9058	− 40.8684	7.4410	7.5044
ANSYS	40.8680	− 7.4412	− 66.9090	− 40.8680	7.4412	7.5032
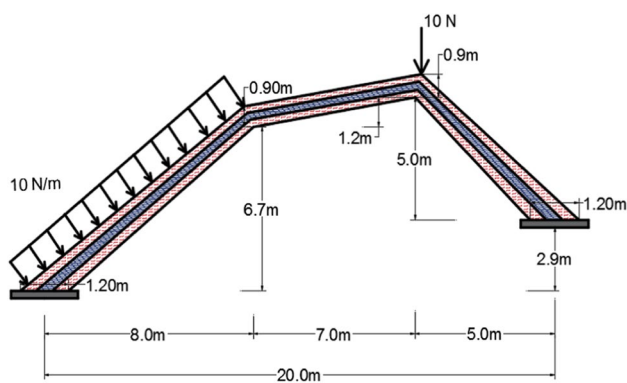
Fig. 7 Frame system containing straight axis elements
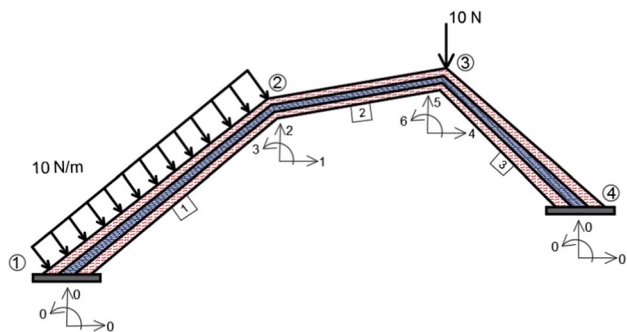

Fig. 8 Degrees of freedom of nodes and code numbers

$$G_{23} = \frac{E_1}{\left(1 + v_{23}\right)} \qquad (46)$$

Tables 7, 8, 9 and 10 represent the results obtained due to analysis of the frame system (Figs. 7 and 8) for E_1/E_2 ratios and KI material properties. The entire layer stacking angle cases (Figs. 9 and 10) are taken into account, and the frame system is solved for each calculated E_1/E_2 ratio separately.

After the results are examined, it is understood that E_1/E_2 ratio highly affects the node displacement values of the system at all layer stacking angles considered for KI material properties.

3.3 Example 3

A composite laminated frame structure is considered as in Figs. 11 and 12. The suggested approach is applied to carry out the influence of the E_1/E_2 on the bending response of the considered frame structures for KII material properties. Results are presented in Tables 11, 12, 13 and 14.

Tables 11, 12, 13 and 14 represent the numerical values of node displacements obtained for each lamination scheme designed for KII material properties. Lamination scheme is considered for 1, 10, 15, 20 and 30 E_1/E_2 ratios as given in Fig. 10. After a careful review of the results presented in the above tables, it is concluded that by increasing the E_1/E_2 ratio, the displacement values are also increasing. As the highest nodal displacement is determined at case III (see Fig. 10) when the E_1/E_2 ratio is 30.

4 Conclusions

An efficient numerical method is used to investigate the effects of fiber angle and E_1/E_2 ratio on the static response of frame systems containing straight and circular axis beam elements carrying in-plane concentrated and uniformly distributed static loads. The TBT is used in the formulations, considering axial and shear deformation effects. Equations governing the static response of the system are first obtained in vector form; in the continuation, for ease of the calculations, the previously obtained equations are transformed to the set of scalar equations. The solution of the set of canonical first-order ordinary differential equations that govern the static behavior of frame systems is

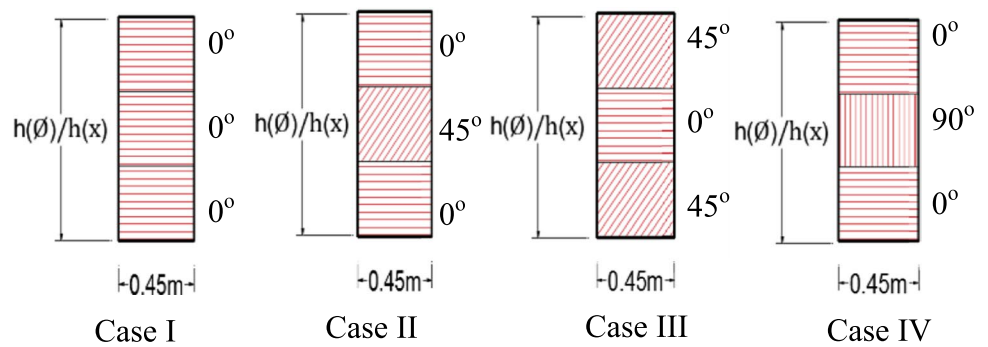**Fig. 9** Cross-sectional layouts for KI material properties

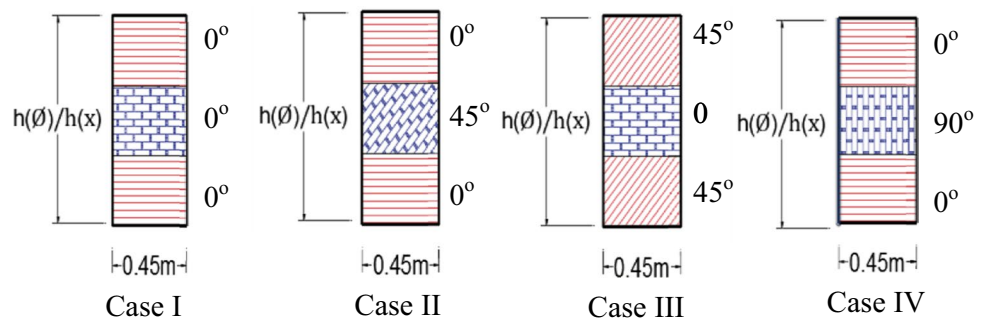**Fig. 10** Cross-sectional layouts for KII material properties

Table 5 Node displacement values for KI materials group

Node number	Stacking sequence	U_i(m)	U_n(m)	Ω_b(Rad.)
2	0° 0° 0°	0.565715E−06	− 0.682477E−06	0.158980E−06
	0° 45° 0°	0.761479E−06	− 0.919320E−06	0.222933E−06
	45° 0° 45°	0.129078E−05	− 0.155935E−05	0.385350E−06
	0° 90° 0°	0.795346E−06	− 0.959850E−06	0.228626E−06
3	0° 0° 0°	0.379600E−06	0.373460E−06	0.130905E−07
	0° 45° 0°	0.510533E−06	0.501713E−06	0.137022E−07
	45° 0° 45°	0.864759E−06	0.848953E−06	0.199075E−07
	0° 90° 0°	0.533466E−06	0.524550E−06	0.161777E−07

Table 6 Node displacement values for KII materials group

Node number	Stacking sequence	U_i(m)	U_n(m)	Ω_b(Rad.)
2	0° 0° 0°	0.671357E−06	− 0.809934E−06	0.188829E−06
	0° 45° 0°	0.790089E−06	− 0.953656E−06	0.228914E−06
	45° 0° 45°	0.211366E−05	− 0.255449E−05	0.634050E−06
	0° 90° 0°	0.815536E−06	− 0.984089E−06	0.232558E−06
3	0° 0° 0°	0.450480E−06	0.443184E−06	0.154654E−07
	0° 45° 0°	0.529845E−06	0.520864E−06	0.152792E−07
	45° 0° 45°	0.141538E−05	0.138859E−05	0.312859E−07
	0° 90° 0°	0.547088E−06	0.538050E−06	0.174086E−07

carried out by the CFM. This method turns the two-point boundary value problems into the set of initial value problems. RK5 algorithm is applied for the solution of the set of initial value problems, and for this purpose, a computer program is coded in Fortran. The accuracy and validation of the coded program are performed with the finite element method.

The problems presented in this study are solved for two cross-sectional layouts of KI and KII material properties separately, while performing the analysis in ANSYS each

Table 7 Effects of E_1/E_2 ratio on displacement values for KI material properties

Stacking sequence	Node	Displacement	E_1/E_2 ratios				
			1	10	15	20	30
0° 0° 0°	2	U_t (m)	5.1264E−07	5.4217E−07	5.5855E−07	5.7491E−07	6.0760E−07
		U_n (m)	−6.1915E−07	−6.5439E−07	−6.7393E−07	−6.9344E−07	−7.3244E−07
		Ω_b (Rad.)	1.5455E−07	1.5702E−07	1.5838E−07	1.5974E−07	1.6245E−07
	3	U_t (m)	3.4353E−07	3.6360E−07	3.7473E−07	3.8584E−07	4.0806E−07
		U_n (m)	3.3739E−07	3.5746E−07	3.6859E−07	3.7970E−07	4.0192E−07
		Ω_b (Rad.)	7.1983E−09	1.0513E−08	1.2312E−08	1.4082E−08	1.7547E−08

Table 8 Effects of E_1/E_2 ratio on displacement values for KI material properties

Stacking sequence	Node	Displacement	E_1/E_2 ratios				
			1	10	15	20	30
0° 45° 0°	2	U_t (m)	5.1264E−07	7.2783E−07	7.5435E−07	7.7348E−07	8.0324E−07
		U_n (m)	−6.1916E−07	−8.7889E−07	−9.1076E−07	−9.3370E−07	−9.6935E−07
		Ω_b (Rad.)	1.5455E−07	2.1550E−07	2.2134E−07	2.2495E−07	2.2964E−07
	3	U_t (m)	3.4354E−07	4.8785E−07	5.0572E−07	5.1864E−07	5.3878E−07
		U_n (m)	3.3739E−07	4.7927E−07	4.9695E−07	5.0977E−07	5.2980E−07
		Ω_b (Rad.)	7.1984E−09	1.2014E−08	1.3355E−08	1.4582E−08	1.6896E−08

Table 9 Effects of E_1/E_2 ratio on displacement values for KI material properties

Stacking sequence	Node	Displacement	E_1/E_2 ratios				
			1	10	15	20	30
45° 0° 45°	2	U_t (m)	5.1264E−07	1.1634E−06	1.2626E−06	1.3255E−06	1.4046E−06
		U_n (m)	−6.1917E−07	−1.4058E−06	−1.5254E−06	−1.6013E−06	−1.6964E−06
		Ω_b (Rad.)	1.5455E−07	3.4852E−07	3.7701E−07	3.9454E−07	4.1541E−07
	3	U_t (m)	3.4354E−07	7.7923E−07	8.4579E−07	8.8809E−07	9.4126E−07
		U_n (m)	3.3739E−07	7.6473E−07	8.3022E−07	8.7191E−07	9.2440E−07
		Ω_b (Rad.)	7.1984E−09	1.7414E−08	1.9447E−08	2.0983E−08	2.3420E−08

Table 10 Effects of E_1/E_2 ratio on displacement values for KI material properties

Stacking sequence	Node	Displacement	E_1/E_2 ratios				
			1	10	15	20	30
0° 90° 0°	2	U_t (m)	5.1264E−07	7.6006E−07	7.8817E−07	8.1054E−07	8.4939E−07
		U_n (m)	−6.1915E−07	−9.1758E−07	−9.5129E−07	−9.7807E−07	−1.0245E−06
		Ω_b (Rad.)	1.5455E−07	2.2310E−07	2.2803E−07	2.3121E−07	2.3578E−07
	3	U_t (m)	3.4353E−07	5.0960E−07	5.2859E−07	5.4373E−07	5.7008E−07
		U_n (m)	3.3739E−07	5.0082E−07	5.1967E−07	5.3475E−07	5.6102E−07
		Ω_b (Rad.)	7.1983E−09	1.3408E−08	1.5386E−08	1.7269E−08	2.0903E−08

element of the frame is divided into 5, 10 and 20 parts. It can be understood from the results presented for the frame systems that increasing the number of divisions for each element provides a fast convergence. After a precise reviewing of the analysis done by the FE-based package program, it can be understood that hundreds of elements should be used to achieve the results with intended sufficient precision, while doing the same analysis by the CFM, in order to achieve the results with the intended precision, it is enough to divide the solution zone into a few elements.
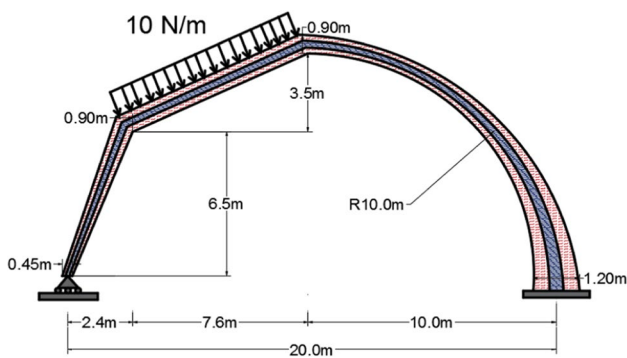
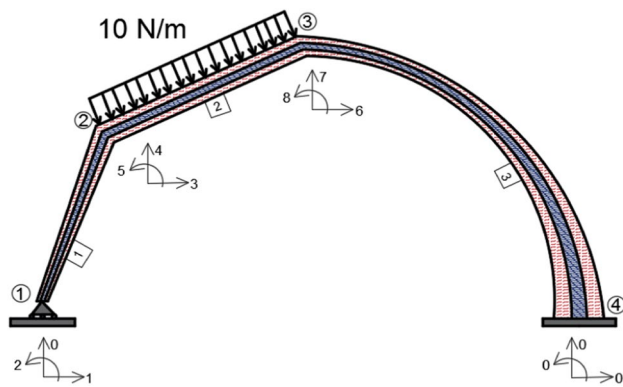**Fig. 11** Frame system containing straight and curved elements

Fig. 12 Degrees of freedom of nodes and code numbers

Four different cross-sectional schemes are designed with different stacking sequences and both KI and KII material properties. The frame system is solved for each cross-sectional layout, and the effects of stacking sequences are examined. Along with the axial and normal displacements the rotations are highly affected by the changes in stacking sequences, and it can be clearly seen from the numerical results presented for KI and KII materials.

In order to study the effects of E_1/E_2 ratio on the node displacements and rotations, five different E_1/E_2 ratios are introduced by keeping the E_1 constant and decreasing the value of E_2. The results obtained from the solution of the problem for each of the composed ratios ($E_1/E_2 = 1$, 10, 15, 20, 30) are examined elaborately. The problem is analyzed for several lamination schemes considering E_1/E_2 ratio from 1 to 30 separately; thus, the effects of E_1/E_2 ratio together with the fiber angles are examined for the frame system. As a result, the maximum displacement values of the system are detected, while the orthotropicity ratio is equal to 30 at case III (45° 0° 45°) cross-sectional layout.

It must be highlighted once again that the main objective of this work is to implement the CFM to the static analysis of composite laminated frames. This framework may be used as a benchmark solution for future studies on the related subject.

Appendix A: Formulations for composite materials

The stress–strain and strain–stress relations for composite materials in 1, 2, 3 coordinate systems are written, respectively, as:

$$\sigma_i = C'_{ij}\varepsilon_j \quad \varepsilon_i = S'_{ij}\sigma_j \quad (i, j = 1, 2, \ldots, 6) \tag{47}$$

In the above relations the notation C'_{ij} and S'_{ij} shows the transformed stiffness and compliance matrices and can be calculated as follows [38, 43].

$$[C'] = [T°]^{-1}[C][\forall][T°][\forall]^{-1}, \quad [S'] = [\forall][T°]^{-1}[\forall]^{-1}[S][T°] \tag{48}$$

The transformation matrices components are defined as

Table 11 Effects of E_1/E_2 ratio on displacement values for KII material properties

Stacking sequence	Node	Displacement	E_1/E_2 ratios				
			1	10	15	20	30
0° 45° 0°	1	U_t (m)	−9.5936E−06	−1.1630E−05	−1.1789E−05	−1.1883E−05	−1.1995E−05
		U_n (m)	0.0000E+00	0.0000E+00	0.0000E+00	0.0000E+00	0.0000E+00
		Ω_b (Rad.)	−1.3638E−06	−1.6517E−06	−1.6734E−06	−1.6858E−06	−1.7001E−06
	2	U_t (m)	−1.9384E−06	−2.3166E−06	−2.3309E−06	−2.3319E−06	−2.3189E−06
		U_n (m)	−2.8346E−06	−3.4485E−06	−3.5022E−06	−3.5364E−06	−3.5828E−06
		Ω_b (Rad.)	−8.5937E−07	−1.0414E−06	−1.0555E−06	−1.0636E−06	−1.0733E−06
	3	U_t (m)	−1.4790E−06	−1.7600E−06	−1.7667E−06	−1.7634E−06	−1.7453E−06
		U_n (m)	−3.8390E−06	−4.6656E−06	−4.7358E−06	−4.7795E−06	−4.8371E−06
		Ω_b (Rad.)	5.3255E−07	6.4274E−07	6.5006E−07	6.5371E−07	6.5691E−07

Table 12 Effects of E_1/E_2 ratio on displacement values for KII material properties

Stacking sequence	Node	Displacement	E_1/E_2 ratios				
			1	10	15	20	30
0° 0° 0°	1	U_t (m)	−9.5937E−06	−9.6274E−06	−9.6461E−06	−9.6648E−06	−9.7023E−06
		U_n (m)	0.0000E+00	0.0000E+00	0.0000E+00	0.0000E+00	0.0000E+00
		Ω_b (Rad.)	−1.3638E−06	−1.3664E−06	−1.3678E−06	−1.3692E−06	−1.3721E−06
	2	U_t (m)	−1.9384E−06	−1.8999E−06	−1.8786E−06	−1.8572E−06	−1.8144E−06
		U_n (m)	−2.8346E−06	−2.8612E−06	−2.8760E−06	−2.8908E−06	−2.9205E−06
		Ω_b (Rad.)	−8.5938E−07	−8.6186E−07	−8.6324E−07	−8.6461E−07	−8.6736E−07
	3	U_t (m)	−1.4790E−06	−1.4393E−06	−1.4172E−06	−1.3951E−06	−1.3509E−06
		U_n (m)	−3.8391E−06	−3.8685E−06	−3.8849E−06	−3.9013E−06	−3.9340E−06
		Ω_b (Rad.)	5.3255E−07	5.3055E−07	5.2944E−07	5.2833E−07	5.2611E−07

Table 13 Effects of E_1/E_2 ratio on displacement values for KII material properties

Stacking sequence	Node	Displacement	E_1/E_2 ratios				
			1	10	15	20	30
45° 0° 45°	1	U_t (m)	−9.5939E−06	−2.8236E−05	−3.1930E−05	−3.4348E−05	−3.7347E−05
		U_n (m)	0.0000E+00	0.0000E+00	0.0000E+00	0.0000E+00	0.0000E+00
		Ω_b (Rad.)	−1.3638E−06	−4.0140E−06	−4.5388E−06	−4.8821E−06	−5.3074E−06
	2	U_t (m)	−1.9384E−06	−5.6946E−06	−6.4331E−06	−6.9133E−06	−7.5016E−06
		U_n (m)	−2.8346E−06	−8.3486E−06	−9.4429E−06	−1.0160E−05	−1.1053E−05
		Ω_b (Rad.)	−8.5940E−07	−2.5295E−06	−2.8603E−06	−3.0768E−06	−3.3452E−06
	3	U_t (m)	−1.4791E−06	−4.3432E−06	−4.9048E−06	−5.2693E−06	−5.7141E−06
		U_n (m)	−3.8391E−06	−1.1305E−05	−1.2786E−05	−1.3757E−05	−1.4963E−05
		Ω_b (Rad.)	5.3257E−07	1.5669E−06	1.7713E−06	1.9048E−06	2.0697E−06

Table 14 Effects of E_1/E_2 ratio on displacement values for KII material properties

Stacking sequence	Node	Displacement	E_1/E_2 ratios				
			1	10	15	20	30
0° 90° 0°	1	U_t (m)	−9.5937E−06	−1.1834E−05	−1.1954E−05	−1.2025E−05	−1.2114E−05
		U_n (m)	0.0000E+00	0.0000E+00	0.0000E+00	0.0000E+00	0.0000E+00
		Ω_b (Rad.)	−1.3638E−06	−1.6802E−06	−1.6960E−06	−1.7048E−06	−1.7150E−06
	2	U_t (m)	−1.9384E−06	−2.3473E−06	−2.3465E−06	−2.3356E−06	−2.3033E−06
		U_n (m)	−2.8346E−06	−3.5127E−06	−3.5575E−06	−3.5874E−06	−3.6323E−06
		Ω_b (Rad.)	−8.5938E−07	−1.0596E−06	−1.0700E−06	−1.0760E−06	−1.0834E−06
	3	U_t (m)	−1.4790E−06	−1.7810E−06	−1.7746E−06	−1.7605E−06	−1.7243E−06
		U_n (m)	−3.8391E−06	−4.7511E−06	−4.8080E−06	−4.8450E−06	−4.8984E−06
		Ω_b (Rad.)	5.3255E−07	6.5318E−07	6.5770E−07	6.5945E−07	6.6010E−07

$$[T°] = \begin{bmatrix} m^2 & n^2 & 0 & 0 & 0 & 2mn \\ n^2 & m^2 & 0 & 0 & 0 & -2mn \\ 0 & 0 & 1 & 0 & 0 & 0 \\ 0 & 0 & 0 & m & -n & 0 \\ 0 & 0 & 0 & n & m & 0 \\ -mn & mn & 0 & 0 & 0 & m^2 - n^2 \end{bmatrix} \qquad (49)$$

in which $m = \cos(\theta)$ and $n = \sin(\theta)$.

$$[\forall] = \begin{bmatrix} 1 & 0 & 0 & 0 & 0 & 0 \\ & 1 & 0 & 0 & 0 & 0 \\ & & 1 & 0 & 0 & 0 \\ & & & 2 & 0 & 0 \\ & \text{Symmetric} & & & 2 & 0 \\ & & & & & 2 \end{bmatrix} \tag{50}$$

A, B, F and D matrices are (3×3) in dimensions and are dependent to the material properties and geometry of the cross section and can be written as follows (see [43] and [50]):

$$A_{ij} = \int_A \tilde{Q}_{ij} \mathrm{d}A \quad B_{ij} = \varepsilon_{mjk} \int_A \tilde{Q}_{im} x_k \mathrm{d}A \tag{51}$$

$$F_{ij} = \varepsilon_{ikm} \int_A x_k \tilde{Q}_{mj} \mathrm{d}A \quad D_{ij} = \varepsilon_{ihk} \varepsilon_{mjp} \int_A x_h x_p \tilde{Q}_{km} \mathrm{d}A \tag{52}$$

In the above equations ε_{ijk} is the permutation tensor and $\tilde{Q}_{ij}$ is reduced stiffness matrix [43].

The transformed stress–strain relations can be written as

$$\tilde{\sigma}_i = \tilde{Q}'_{ij} \tilde{\varepsilon}_j \quad (i, j = 1, 2, \ldots, 6) \tag{53}$$

in which the $\tilde{Q}'_{ij}$ show the reduced and transformed stiffness matrix. The nonzero elements of $\tilde{Q}'_{ij}$ are obtained in terms of the general three-dimensional transformed stiffness and compliance matrices.

$$\tilde{Q}'_{11} = C'_{11} + \left(C'_{12} S'_{12} + C'_{13} S'_{31} \right) \alpha'_{11} + \left(C'_{12} S'_{26} + C'_{13} S'_{36} \right) \alpha'_{61} \tag{54}$$

$$\tilde{Q}'_{12} = C'_{16} + \left(C'_{12} S'_{21} + C'_{13} S'_{31} \right) \alpha'_{16} + \left(C'_{12} S'_{26} + C'_{13} S'_{36} \right) \alpha'_{66} \tag{55}$$

$$\tilde{Q}'_{22} = C'_{66} + \left(C'_{62} S'_{21} + C'_{63} S'_{31} \right) \alpha'_{16} + \left(C'_{62} S'_{26} + C'_{63} S'_{36} \right) \alpha'_{66} \tag{56}$$

$$\tilde{Q}'_{22} = C'_{55} \tag{57}$$

$$\alpha'_{11} = \frac{S'_{66}}{S'_{11} S'_{66} - S'^2_{16}} \quad \alpha'_{16} = \alpha'_{61} = \frac{-S'_{66}}{S'_{11} S'_{66} - S'^2_{16}} \quad \alpha'_{66} = \frac{S'_{11}}{S'_{11} S'_{66} - S'^2_{16}} \tag{58}$$

The transformed stiffness and compliance matrices for an orthotropic material are obtained in the following form.

$$[C'] = \begin{bmatrix} C'_{11} & C'_{12} & C'_{13} & 0 & 0 & C'_{16} \\ C'_{21} & C'_{22} & C'_{23} & 0 & 0 & C'_{26} \\ C'_{31} & C'_{32} & C'_{33} & 0 & 0 & C'_{36} \\ 0 & 0 & 0 & C'_{44} & C'_{45} & 0 \\ 0 & 0 & 0 & C'_{54} & C'_{55} & 0 \\ C'_{61} & C'_{62} & C'_{63} & 0 & 0 & C'_{66} \end{bmatrix} \tag{59}$$

$$[S'] = \begin{bmatrix} S'_{11} & S'_{12} & S'_{13} & 0 & 0 & S'_{16} \\ S'_{21} & S'_{22} & S'_{23} & 0 & 0 & S'_{26} \\ S'_{31} & S'_{32} & S'_{33} & 0 & 0 & S'_{36} \\ 0 & 0 & 0 & S'_{44} & S'_{45} & 0 \\ 0 & 0 & 0 & S'_{54} & S'_{55} & 0 \\ S'_{61} & S'_{62} & S'_{63} & 0 & 0 & S'_{66} \end{bmatrix} \tag{60}$$

The nonzero components of the transformed stiffness matrix are obtained as follows

$$C'_{11} = m^4 C_{11} + 2n^2 m^2 C_{12} + n^4 C_{22} + 4n^2 m^2 C_{66} \tag{61}$$

$$C'_{12} = n^2 m^2 C_{11} + \left(n^4 + m^4 \right) C_{12} + n^2 m^2 C_{22} - 4n^2 m^2 C_{66} \tag{62}$$

$$C'_{13} = m^2 C_{13} + n^2 C_{23} \tag{63}$$

$$C'_{16} = nm^3 C_{11} + nm \left(n^2 - m^2 \right) C_{12} - n^3 m C_{22} + 2nm \left(n^2 - m^2 \right) C_{66} \tag{64}$$

$$C'_{22} = n^4 C_{11} + 2n^2 m^2 C_{12} + m^4 C_{22} + 4n^2 m^2 C_{66} \tag{65}$$

$$C'_{23} = n^2 C_{13} + m^2 C_{23} \tag{66}$$

$$C'_{26} = nm^3 C_{11} + nm \left(m^2 - n^2 \right) C_{12} - nm^3 C_{22} - 2nm \left(m^2 - n^2 \right) C_{66} \tag{67}$$

$$C'_{33} = C_{33} \tag{68}$$

$$C'_{36} = nm C_{13} - nm C_{23} \tag{69}$$

$$C'_{44} = m^2 C_{44} + n^2 C_{55} \tag{70}$$

$$C'_{45} = -nm C_{44} + nm C_{55} \tag{71}$$

$$C'_{55} = n^2 C_{44} + m^2 C_{55} \tag{72}$$

$$C'_{66} = n^2 m^2 C_{11} - 2n^2 m^2 C_{12} + n^2 m^2 C_{22} + \left(m^2 - n^2 \right)^2 C_{66} \tag{73}$$

The nonzero components of the compliance matrix are obtained in the following form.

$$S'_{11} = m^4 S_{11} + 2n^2 m^2 S_{12} + n^4 S_{22} + n^2 m^2 S_{66} \tag{74}$$

$$S'_{12} = n^2 m^2 S_{11} + \left(n^4 + m^4 \right) S_{12} + n^2 m^2 S_{22} - n^2 m^2 S_{66} \tag{75}$$

$$S'_{13} = m^2 S_{13} + n^2 S_{23} \tag{76}$$

$$S'_{16} = 2nm^3 S_{11} + 2nm(n^2 - m^2)S_{12} - 2n^3 m S_{22} + nm(n^2 - m^2)S_{66} \tag{77}$$

$$S'_{22} = n^4 S_{11} + 2n^2 m^2 S_{12} + m^4 S_{22} + n^2 m^2 S_{66} \tag{78}$$

$$S'_{23} = n^2 S_{13} + m^2 S_{23} \tag{79}$$

$$S'_{26} = 2n^3 m S_{11} + 2nm(m^2 - n^2)S_{12} - 2nm^3 S_{22} + nm(m^2 - n^2)S_{66} \tag{80}$$

$$S'_{33} = S_{33} \tag{81}$$

$$S'_{36} = 2nm S_{13} - 2nm S_{23} \tag{82}$$

$$S'_{44} = m^2 S_{44} + n^2 S_{55} \tag{83}$$

$$S'_{45} = -nm S_{44} + nm S_{55} \tag{84}$$

$$S'_{55} = n^2 S_{44} + m^2 S_{55} \tag{85}$$

$$S'_{66} = 4n^2 m^2 S_{11} - 8n^2 m^2 S_{12} + 4n^2 m^2 S_{22} + (m^2 - n^2)^2 S_{66} \tag{86}$$

$\boldsymbol{B} = \boldsymbol{F} = 0$ relation is valid for symmetric laminates.

The nonzero elements of $\boldsymbol{A}$ and $\boldsymbol{D}$ matrices are given in the following equations.

$$A_{11} = \sum_{k=1}^{N} \tilde{Q}'^{(k)}_{11} A^{(k)} \quad A_{12} = \sum_{k=1}^{N} \tilde{Q}'^{(k)}_{12} A^{(k)} \tag{87}$$

$$A_{22} = \sum_{k=1}^{N} \tilde{Q}'^{(k)}_{22} A^{(k)} \quad A_{33} = \sum_{k=1}^{N} \tilde{Q}'^{(k)}_{33} A^{(k)} \tag{88}$$

$$D_{11} = \sum_{k=1}^{N} \tilde{Q}'^{(k)}_{33} I_3^{(k)} + \sum_{k=1}^{N} \tilde{Q}'^{(k)}_{22} I_2^{(k)} \tag{89}$$

$$D_{12} = -\sum_{k=1}^{N} \tilde{Q}'^{(k)}_{21} I_2^{(k)} \tag{90}$$

$$D_{22} = \sum_{k=1}^{N} \tilde{Q}'^{(k)}_{11} I_2^{(k)} \quad D_{33} = \sum_{k=1}^{N} \tilde{Q}'^{(k)}_{11} I_3^{(k)} \tag{91}$$

The nonzero elements of the transformed $\boldsymbol{A}'$ and $\boldsymbol{D}'$ matrices are calculated by using the following equations.

$$A'_{11} = \frac{A_{22}}{A_{11}A_{22} - A_{12}^2} \quad A'_{12} = -\frac{A_{12}}{A_{11}A_{22} - A_{12}^2} \tag{92}$$

$$A'_{22} = \frac{A_{11}}{A_{11}A_{22} - A_{12}^2} \quad A'_{33} = \frac{1}{A_{33}} \tag{93}$$

$$D'_{11} = \frac{D_{22}}{D_{11}D_{22} - D_{12}^2} \quad D'_{12} = -\frac{D_{12}}{D_{11}D_{22} - D_{12}^2} \tag{94}$$

$$D'_{22} = \frac{D_{11}}{D_{11}D_{22} - D_{12}^2} \quad D'_{33} = \frac{1}{D_{33}} \tag{95}$$

Compliance with ethical standards

Conflict of interest The authors declare that they have no conflict of interest.

References

1. Vo TP, Thai HT (2012) Static behavior of composite beams using various refined shear deformation theories. Compos Struct 94(8):2513–2522
2. Ditaranto RA (1973) Static analysis of a laminated beam. J Eng Ind Trans ASME 95:755–761
3. Reddy JN, Wang CM, Lee KH (1997) Relationships between bending solutions of classical and shear deformation beam theories. Int J Solids Struct 34(26):3373–3384
4. Karamanlı A (2017) Bending analysis of composite and sandwich beams using Ritz method. Anadolu Univ J Sci Technol A Appl Sci Eng 19(1):10–23
5. Catapano A, Giunta G, Belouettar S, Carrera E (2011) Static analysis of laminated beams via a unified formulation. Compos struct 94(1):75–83
6. Özütok A, Madenci E (2017) Static analysis of laminated composite beams based on higher-order shear deformation theory by using mixed-type finite element method. Int J Mech Sci 130:234–243
7. Pagani A, Yan Y, Carrera E (2017) Exact solutions for static analysis of laminated, box and sandwich beams by refined layer-wise theory. Compos Part B Eng 131:62–75
8. Ecsedi I, Baksa A (2011) Static analysis of composite beams with weak shear connection. Appl Math Model 35(4):1739–1750
9. Aguiar RM, Moleiro F, Soares CM (2012) Assessment of mixed and displacement-based models for static analysis of composite beams of different cross-sections. Compos Struct 94(2):601–616
10. Eisenberger M (2003) An exact high order beam element. Comput Struct 81(3):147–152
11. Khdeir AA, Reddy JN (1997) An exact solution for the bending of thin and thick cross-ply laminated beams. Compos Struct 37(2):195–203
12. Yuan FG, Miller RE (1990) A higher order finite element for laminated beams. Compos Struct 14(2):125–150
13. Yu H (1994) A higher-order finite element for analysis of composite laminated structures. Compos Struct 28(4):375–383
14. Vo TP, Thai HT, Nguyen TK, Lanc D, Karamanli A (2017) Flexural analysis of laminated composite and sandwich beams using

a four-unknown shear and normal deformation theory. Compos Struct 176:388–397

15. Cunedioğlu Y (2017) Statics and buckling analysis of aluminum beams with composite coats. Omer Halisdemir Univ J Eng Sci 6(2):729–736

16. Masjedi PK, Weaver PM (2020) Analytical solution for the fully coupled static response of variable stiffness composite beams. Appl Math Model 81:16–36

17. Daví G, Milazzo A, Orlando C (2014) An analytical solution for multilayered beams subjected to ends loads. Compos Struct 116:772–781

18. Vukasović M, Pavazza R, Vlak F (2017) An analytic solution for bending of thin-walled laminated composite beams of symmetrical open sections with influence of shear. J Strain Anal Eng Des 52(3):190–203

19. Saraçoğlu M, Güçlü G, Fethullah USLU (2019) Static analysis of orthotropic Euler–Bernoulli and Timoshenko beams with respect to various parameters. Bitlis Eren Univ J Sci 8(2):628–641

20. Elshafei MA (2013) FE Modeling and analysis of isotropic and orthotropic beams using first order shear deformation theory. Mater Sci Appl 4:77–102

21. Zghal S, Ataoui D, Dammak F (2020) Static bending analysis of beams made of functionally graded porous materials. Mech Based Des Struct Mach. https://doi.org/10.1080/15397734.2020.1748053

22. Doeva O, Khaneh Masjedi P, Weaver PM (2020) Exact solution for the deflection of composite beams under non-uniformly distributed loads. In: AIAA Scitech 2020 Forum, p 0245

23. Noori AR, Aslan TA, Temel B (2020) Static analysis of FG beams via complementary functions method. Eur Mech Sci 4(1):1–6

24. Mathiyazhagan G, Vasiraja N (2013) Finite element analysis on curved beams of various sections. In: 2013 International conference on energy efficient technologies for sustainability. IEEE, pp 168–173

25. Barhate BR, Waghe UP (2016) Static analysis of composite laminated beam by first order shear deformation theory. Int J Eng Appl Sci 3(11):257559

26. Alaimo A, Davì G, Milazzo A, Orlando C (2017) Analytical solution for composite layered beam subjected to uniformly distributed load. Mech Adv Mater Struct 24(16):1315–1324

27. Sayyad AS, Ghugal YM, Naik NS (2015) Bending analysis of laminated composite and sandwich beams according to refined trigonometric beam theory. Curved Layered Struct. https://doi.org/10.1515/cls-2015-001

28. Pandey N, Gadade AM (2019) Static response of laminated composite beam subjected to transverse loading. Mater Today Proc 16:956–963

29. Ghugal ASY (2011) Effect of transverse shear and transverse normal strain on bending analysis of cross-ply laminated beams. Int J Appl Math Mech 7(12):85–118

30. Rasooli H, Temel B (2019) Static analysis of frames consisting straight and circular axis beams with a variable cross-section made of laminated composite materials by the complementary functions method. Omer Halisdemir Univ J Eng Sci 8(3):046–056 ((in Turkish))

31. Ghugal YM, Shinde SB (2013) Flexural analysis of cross-ply laminated beams using layerwise trigonometric shear deformation theory. Latin Am J Solids Struct 10(4):675–705

32. Aslan TA, Noori AR, Temel B (2017) Static analysis of the circular structural elements with the complementary functions method. Çukurova Univ J Fac Eng Archit 32(1):23–29 ((in Turkish))

33. Karacam F, Timarci T (2005) Bending of cross-ply beams with different boundary conditions. In: International scientific conference, 24–25 November 2005, GABROVO

34. Madenci E, Özkılıç YO, Gemi L (2020) Experimental and theoretical investigation on flexure performance of pultruded GFRP composite beams with damage analyses. Compos Struct 242:112162

35. Madenci E, Özütok A (2017) Variational approximate and mixed-finite element solution for static analysis of laminated composite plates. Solid State Phenom 267:35–39

36. Madenci E, Özütok A (2020) Variational approximate for high order bending analysis of laminated composite plates. Struct Eng Mech 73(1):97–108

37. Temel B, Noori AR (2019) Out-of-plane vibrations of shear-deformable AFG cycloidal beams with variable cross section. Appl Acoust 155:84–96

38. Çalım FF (2003) Dynamic analysis of viscoelastic, anisotropic curved spatial rod systems. PhD. Thesis, University of Cukurova, Adana, **(In Turkish)**

39. Noori AR, Aslan TA, Temel B (2021) dynamic analysis of functionally graded porous beams using complementary functions method in the Laplace domain. Compos Struct 256:113094

40. Yildirim S (2020) Hydrogen elasticity solution of functionally-graded spheres, cylinders and disks. Int J Hydrog Energy 45(41):22094–22101

41. Yildirim S (2020) Free vibration analysis of sandwich beams with functionally-graded cores by complementary functions method. AIAA J 12:1–9

42. Temel B, Aslan TA, Noori AR (2017) An efficient dynamic analysis of planar arches. Eur Mech Sci 1(3):82–88

43. Noori AR, Temel B (2020) On the vibration analysis of laminated composite parabolic arches with variable cross-section of various ply stacking sequences. Mech Adv Mater Struct 27(19):1658–1672

44. Jamil H, Tutuncu N (2019) Numerical methods in calculating eigenvalues: case studies in stability of Euler columns. ALKU J Sci 1(3):156–164

45. ANSYS, Inc Release 15.0, Canonsburg, PA 2013

46. Rasooli H (2020) Static analysis of composite circular and straight axis beam systems by the complementary functions method (published). MSC Thesis, Cukurova University, Adana, Turkey

47. Mechanical APDL element reference. Inc., 275 Technology Drive, Canonsburg, PA15317, 2013

48. Mechanical APDL theory reference. Inc., 275 Technology Drive, Canonsburg, PA15317, 2013

49. Hull D, Clyne TW (1996) An introduction to composite materials. Cambridge solid state science series

50. Jones RM (1999) Mechanics of COMPOSITE MATERIALS. Taylor & Francis. Inc., USA